

## Molecular Composition Dynamics and Structure of Cocoa Butter

Rodrigo Campos,<sup>†</sup> Michel Ollivon,<sup>§</sup> and Alejandro G. Marangoni<sup>\*,†</sup><sup>†</sup>Department of Food Science, University of Guelph, Guelph, Canada, N1G 2W1, and <sup>§</sup>Université Paris-Sud, Centre d'Études Pharmaceutiques, Laboratoire de Physico-Chimie des Systèmes Polyphases, UMR CNRS 8612, Châtenay-Malabry Cedex, France

Received July 22, 2009; Revised Manuscript Received October 29, 2009

**ABSTRACT:** The present study endeavors to understand how small changes in the composition of cocoa butter affect its crystal habit, crystallization behavior, microstructure, and mechanical properties. Such compositional variations were attained by blending cocoa butter with 1 and 5% 1,2,3-tristearoyl-glycerol (SSS) or 1,2,3-trilinoleoyl-glycerol (LLL). Structural parameters such as crystallization kinetics, crystal structure, microstructure, and mechanical strength were obtained via differential scanning calorimetry (DSC), pulsed nuclear magnetic resonance (pNMR), X-ray diffraction (XRD), polarized light microscopy (PLM), and texture analysis. Changes in the triacylglycerol (TAG) profile of cocoa butter affected its crystal structure and therefore its functionality. The high melting saturated SSS becomes rapidly undercooled, reducing cocoa butter's onset crystallization times and temperatures. SSS molecules are spatially bigger (i.e., straighter) relative to cocoa butter's symmetric monounsaturated TAG (the unsaturated oleic acid in the sn-2 position introduces a kink into the TAG structure), and hence infringe upon the order of the crystal domain, reducing the crystal–melt interfacial tension, and delaying polymorphic transformations. On the other hand, the limited molecular compatibility between cocoa butter's TAGs and the fully unsaturated low melting LLL prevents it from co-crystallizing with the bulk of cocoa butter's TAGs, only slightly affecting the crystallization behavior, increasing the liquid fraction, having no impact on crystal structure yet accelerating polymorphic transformations into the stable  $\beta$  form.

## Introduction

The physical, thermal, and mechanical properties of many food systems dictate their functional and sensory characteristics, ultimately impacting consumer acceptance. Essential attributes in fat-based products are determined by the different levels of structure within the crystal network, which are formed by their constituent lipid species.<sup>1,2</sup> For example, the distinctive texture, snap, gloss, and melting character of chocolate are dictated by the chemical composition and crystal habit of cocoa butter. Crystal habit includes the polymorphism of the solid state, crystallite size and shape, and spatial distribution of network mass. Furthermore, the solid fat fraction and crystal habit of cocoa butter are greatly affected by heat, mass, and momentum transfer conditions during the tempering process that is used in the manufacture/crystallization of chocolate.

Cocoa butter has been widely studied in terms of its composition,<sup>3,4</sup> polymorphism,<sup>5–7</sup> microstructure,<sup>8,9</sup> and processing.<sup>10–13</sup> A number of authors have undertaken the challenge of relating cocoa butter's chemical composition to its different levels of structure. The polymorphism, molecular compatibility, and phase behavior of pure triacylglycerols (TAG) typically found in cocoa butter [i.e., 1,3-dipalmitoyl-2-oleoyl-glycerol (POP), 1-palmitoyl-2-oleoyl-3-stearoyl-glycerol (POS), and 1,3-stearoyl-2-oleoyl-glycerol (SOS)] have been reported by Sato and co-workers.<sup>13–15</sup> Additionally, studies on the crystallization and phase behavior of other TAGs naturally found in cocoa butter, albeit in minor concentrations, include binary mixtures of 1,2,3-trioleoyl-glycerol

(OOO) and 1,2,3-tripalmitoyl-glycerol (PPP),<sup>16</sup> PPP and POP,<sup>17,18</sup> and POP and 1-palmitoyl-2,3-dioleoyl-glycerol (POO).<sup>19</sup>

Alternative examinations have considered cocoa butter and other natural edible fats (i.e., milk fat and vegetable oils) as distinct lipid components rather than complex mixtures of different TAGs. Crystallization, phase behavior, polymorphism, microstructure, and rheology of different fat blends have been reported. Examples include blending cocoa butter with confectionery fats of different symmetrical monounsaturated TAG's content,<sup>20–22</sup> olive oil,<sup>23</sup> soybean oil or canola oil,<sup>22–25</sup> a high melting fraction of milk fat and sunflower oil,<sup>26</sup> hydrogenated canola oil and soy bean oil,<sup>27</sup> and PPP mixed with sesame oil,<sup>28,29</sup> and butter fat.<sup>30</sup>

The present study considers pure TAGs blended with a natural fat, an intermediate approach that has heretofore not been undertaken. Slight changes in the concentration of saturated or unsaturated TAGs present in commercially available cocoa butter have been made via the addition of either 1,2,3-tristearoyl-glycerol (SSS) or 1,2,3-trilinoleoyl-glycerol (LLL). The objective of this work is to study how small changes in the composition of cocoa butter affect its different levels of structure, from crystal habit and crystallization behavior to microstructure and mechanical properties. For this, the concentration of saturated/unsaturated fatty acids in natural cocoa butter was modified through the addition of up to 5% wt/wt SSS or LLL, and their different levels of structures were studied.

## Materials and Methods

**Model System.** Blends (w/w) of refined cocoa butter (Qzina Specialty Foods Inc., Toronto, ON, Canada) and 1% or 5% either 1,2,3-trilinoleoyl-glycerol (LLL)

\*Corresponding author. Address: Department of Food Science, University of Guelph, 50 Stone Road East, Guelph, Ontario, Canada, N1G 2W1. Phone: +1-519-824-4120 x 54340; fax: +1-519-824-6631; e-mail: amarango@uoguelph.ca.

(99% purity, Sigma-Aldrich Canada Ltd., Oakville, ON, Canada) or 1,2,3-tristearoyl-glycerol (SSS) (91% purity, Acros Organics, NJ, USA) were made. For all analytical determinations, the blends were melted at 80 °C for 30 min to ensure that all crystal memory was erased prior to their static crystallization at 20 and 24 °C.

**Crystallization Kinetics.** The kinetics of crystallization were monitored by measuring the exothermic heat evolved upon crystallization by differential scanning calorimetry (DSC). Onset crystallization temperatures ( $T_{\text{onset}}$ ) were obtained using a DSC 2910 (DuPont Instruments, Willington DE, USA). Five to ten milligrams of sample were placed in DSC pans, hermetically sealed, and transferred to the DSC cell. The sample was first melted at 80 °C for 30 min, after which it was cooled to 0 °C at a rate of 5 °C/min, and kept at 0 °C for 30 min. The temperature at which the heat flow deviated from the baseline, which corresponds to the temperature at which the first crystallites are formed ( $T_{\text{onset}}$ ), was obtained from the resulting thermograms using TA Instruments Universal Analysis 2000 V4.2E software (TA Instruments, Mississauga ON, Canada). The crystallization process as a whole was studied by measuring the heat flow that results from crystallization events with a Microcalix (DSC coupled with a X-ray diffraction (XRD)), as described below.

**Crystal Structure. X-ray Diffraction.** A Microcalix (a high resolution XRD transmission instrument coupled with a DSC) was used to study the polymorphism of the sample blends, while measuring the heat flux that resulted from the crystallization process. The Microcalix was developed in the Laboratory for Physical Chemistry of Polyphasic Systems, at the University of Paris-South in Châtenay – Malabry, France.<sup>31</sup> The coupled XRD recorded simultaneously at both small ( $q = 0\text{--}0.45 \text{ \AA}^{-1}$ ) and wide ( $q = 1.1\text{--}2.1 \text{ \AA}^{-1}$ ) angles through two position sensitive gas linear detectors placed at 177 and 30 cm, respectively, from the sample. The detector channels were calibrated to express the collected XRD data as a function of the scattering vector  $q \text{ (\AA}^{-1}\text{)}$ , where

$$q = \frac{4\pi \sin \theta}{\lambda} = \frac{2\pi}{d} \quad (1)$$

$\theta$  (°) is the angle of incidence of X-rays relative to the crystalline plane,  $\lambda$  is the X-ray wavelength, and  $d$  (Å) is the repetition distance between two planes. The detectors were calibrated with high-purity SSS. The DSC was calibrated with lauric acid.

Glass capillary tubes ( $1.4 \pm 1$  mm diameter and 80 mm long) were filled with the molten fat blends with the aid of a specially developed syringe in order to fill the lower 15 mm of the capillary. This level of filling corresponds to an average sample size of 20 mg. Samples were melted in an oven at 80 °C for 30 min and placed in the sample holder. The sample holder was preset to 60 °C. Immediately after sample insertion, the sample holder was cooled to either 20 or 24 °C at a rate of 5 °C/min, and subsequently held at the temperature of study for isothermal crystallization. An XRD pattern was obtained after acquiring diffraction data for a period of 200 s in the case of samples crystallized at 20 °C, and 1200 s for samples crystallized at 24 °C. A total of 32 consecutive patterns were obtained during each run. During the duration of the experiment the DSC acquired data every 3 s. Measurements were also taken after 1, 2, 3, and 7 days of isothermal storage at each temperature by acquiring XRD data for 1200 s under isothermal conditions.

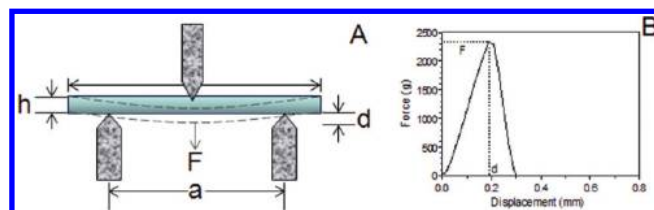


**Figure 1.** Schematic representation of the three point bend determination (A) where the force ( $F$ ) necessary to break a disk with specific diameter ( $b$ ) and height ( $h$ ) of crystallized fat and its resulting deformation to the point of fracture ( $d$ ) are measured. With these experimental settings, a plot of force as a function of the sample displacement is obtained (B) where the yield force ( $F$ ) and the deformation upon fracture ( $d$ ) were calculated.

**Microscopy.** The microstructure of the blends was imaged by polarized light microscopy (PLM). One droplet of molten sample was placed on a pretempered (at 80 °C) glass slide, using a pretempered capillary tube. A pretempered glass coverslip was carefully placed over the sample. The coverslip was placed parallel to the plane of the microscope slide and centered on the drop of sample to ensure a uniform thickness and prevent the formation of air bubbles. The prepared samples were then transferred to temperature controlled incubators set at 20 and 24 °C for static crystallization. At different time points, the prepared samples were placed on a Linkam LTS 350 temperature-controlled microscope stage (Linkam Scientific Instruments, Surrey, UK), set at either 20 or 24 °C. The microstructure was viewed using an Olympus BHA light microscope (Olympus America Ltd., Melville NY, USA). Images were recorded using a Sony XC-75 CCD video camera (Sony Corporation, Japan) with the gain switch in auto position. Images were digitized using Scion Image software (Scion Corporation, Fredrick, MD, USA). Two slides were prepared for each blend, and at least three micrographs were obtained from each slide at each time point. Qualitative observations were made.

**Solid Fat Content.** Approximately 3 g of each fat blend were placed in glass pulsed nuclear magnetic resonance (pNMR) tubes (10 mm diameter, 1 mm thickness, and 180 mm height), melted at 60 °C for 30 min to ensure all crystal memory was erased, and transferred to a water bath set at 20 or 24 °C. Solid fat content (SFC) readings were obtained after 24 and 48 h of isothermal static crystallization using a Bruker PC/20 series pNMR analyzer (Bruker, Milton, ON, Canada). Two sample tubes were measured for each fat blend.

**Mechanical Properties.** The mechanical strength of the fat blends was measured by breaking sample disks and obtaining the force necessary to cause such fracture. Sample disks (20 mm diameter and 3.2 mm height) were prepared by pouring the melted blends into pretempered (at 20 and 24 °C) PVC molds and allowing them to crystallize statically in temperature controlled incubators. A 1122 Instron machine (Instron Canada, Burlington, ON, Canada) with a 1000 lb load cell and a three point bending geometry was used to measure the breaking force of the crystallized samples. With a three point bending geometry, the sample disk is positioned over two points and a third point impinges a constant force in the middle of the sample disk to the point of fracture, as illustrated in Figure 1. The force ( $F$ ) necessary to break the sample disks at a speed of 50 mm/min, as well as the deformation of the disks to the point of fracture ( $d$ ), was calculated with the Instron Series IX Automated Materials

Tester V.9.09.00 software (Instron Canada, Burlington, ON, Canada). With the obtained experimental data, along with the height ( $h$ ) and diameter ( $b$ ) of the disk, and the separation between the two supporting points ( $a$ ), the bending elastic modulus ( $E_B$ ) was calculated using eq 2.<sup>32</sup>

$$E_B = \frac{Fa^3}{4dbh^3} \quad (2)$$

## Results

**Crystallization Kinetics.** Cocoa butter is composed primarily of TAGs containing predominantly palmitic (C16:0), stearic (C18:0), and oleic C18:1 *cis*9 fatty acids. The majority of TAGs in cocoa butter are symmetrical mono-unsaturated, with POP, SOS, and POS being the most predominant.<sup>4</sup> Melting points for these glycerides range between 23.5–43.0 °C for SOS and 15.2–36.7 °C for POP, depending on the polymorphic form.<sup>13</sup> In addition, cocoa butter contains minor quantities of trisaturated as well as di- and triunsaturated TAGs such as triolein OOO, tripalmitin PPP, and tristearin SSS. In the  $\alpha$  polymorphic form, their melting points are −31 °C, 44.7 °C, and 54.9 °C, respectively.<sup>33</sup> With such chemical makeup, cocoa butter has a melting range of 29–34 °C when crystallized in the stable  $\beta$  polymorph.<sup>9,34</sup> Thus, the addition of specific TAGs to cocoa butter can potentially alter the saturation conditions of the melt and consequently affect its crystallization behavior. In this study, highly saturated SSS and highly

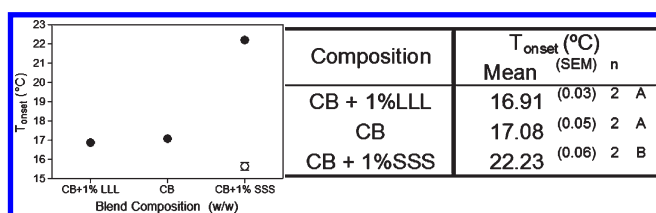


**Figure 2.** Onset crystallization temperature ( $T_{\text{onset}}$ ) of cocoa butter, and cocoa butter samples enriched with 1% (w/w) of LLL or SSS determined by DSC. Samples were melted to 80 °C for 30 min and subsequently cooled to 0 °C at a rate of 5 °C/min. The temperature at which the heat flow deviates from baseline corresponds to  $T_{\text{onset}}$ . Full symbols correspond to an initial crystallization event; empty symbols correspond to the crystallization of a second fraction. Letters indicate significance ( $P < 0.05$ ).

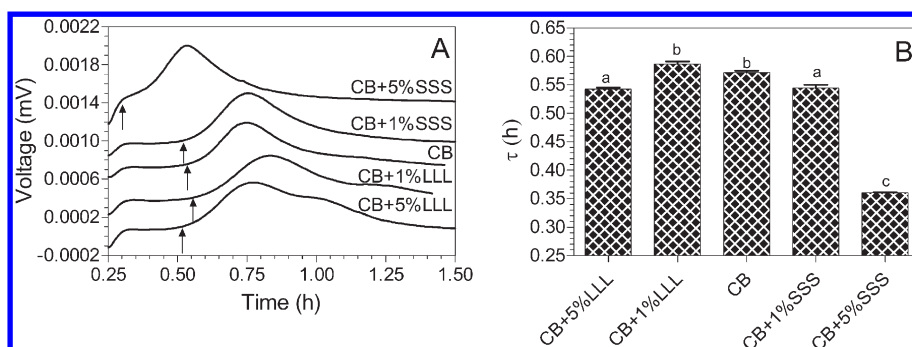


**Figure 3.** Crystallization of cocoa butter blends at 20 °C studied by DSC. The crystallization curves (A) were obtained by melting the samples at 80 °C for 30 min and subsequently cooling to 20 at 5 °C/min. The crystallization curves were constructed with data collected once the DSC cell had reached thermal stability at 20 °C. Induction times of crystallization ( $\tau$ ) (B) were obtained from the crystallization curves by extrapolating the linear increase in voltage to the signal baseline (indicated by arrows in the crystallization curves). Letters denote significant differences ( $P < 0.05$ ).

unsaturated LLL were added to cocoa butter in order to affect its crystallization behavior and structure.

The  $T_{\text{onset}}$  of cocoa butter and cocoa butter enriched with 1% of LLL or SSS are shown in Figure 2. Cocoa butter has a  $T_{\text{onset}}$  of 17 °C. The addition of only 1% liquid oil in the form of low melting LLL did not affect the crystallization behavior of cocoa butter as reflected by the lack of a significant change in  $T_{\text{onset}}$ . On the other hand, the addition of only 1% highly saturated SSS had a considerable effect on cocoa butter's crystallization behavior.  $T_{\text{onset}}$  increased by  $\sim 5$  °C, along with the appearance of a second crystallization event at 15.6 °C. It is possible that the undercooled molecules of SSS induce fractional crystallization by forming a mixed crystal with other high melting point molecules naturally present in cocoa butter, producing a high melting fraction which crystallizes at 22 °C. With further cooling, a second lower melting point fraction subsequently crystallizes at 15.6 °C.

Figure 3 illustrates the changes in isothermal heat flow as a function of time that result from the crystallization of the studied cocoa butter blends at 20 °C. From the curves, the induction time for crystallization ( $\tau$ ) was calculated by extrapolating the linear increase in voltage to the signal baseline. Acquired XRD data yields information relevant to the samples' polymorphic dynamics. This data will be discussed in further detail later in this paper; however, for the interpretation of the data presented in Figure 3, it is important to briefly describe the polymorphic forms present during the first hour of crystallization. There is evidence that upon static crystallization of cocoa butter at 20 °C, the unstable  $\alpha$  polymorph initially forms between 2 and 5 min after the sample has reached isothermal conditions. After 37 min of isothermal storage, a second crystallization event takes place, corresponding to the formation of the  $\beta'$  phase via solid-state transformation of the  $\alpha$  phase.<sup>7</sup> This indicates that the values of  $\tau$  obtained from the thermograms correspond to the crystallization of the  $\beta'$  form, rather than the initial nucleation events. The crystallization of the  $\alpha$  form could not be observed with calorimetry as it takes place early on during the crystallization, when — under the conditions used in this experiment — the DSC cell has just reached isothermal equilibrium.

Upon analysis of crystallization at 20 °C, all blends had  $\tau$  in the range of 0.55 and 0.60 h, with the exception of cocoa butter with added 5% SSS which had a considerably lower  $\tau$  of 0.36 h. The addition of 5% SSS accelerates the overall



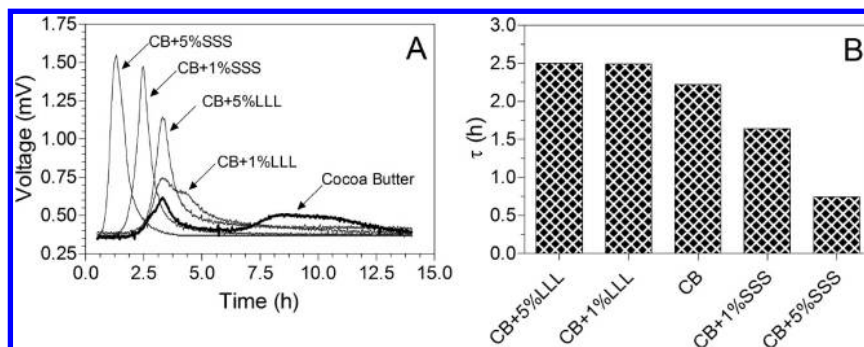


**Figure 4.** Crystallization of cocoa butter blends at 24 °C studied by DSC. The crystallization curves (A) were obtained by melting the samples at 80 °C for 30 min and subsequently cooling to 24 at 5 °C/min. The crystallization curves were constructed with data collected once the DSC cell had reached thermal stability at 24 °C. Each curve was normalized with respect to its total area. Induction times of crystallization ( $\tau$ ) (B) were calculated by extrapolating the linear increase in voltage to the signal baseline.

rate of crystallization, as well as the formation of the  $\beta'$  polymorph. One can notice in Figure 3 that there are two different fractions crystallizing, observed as a change of slope of the cocoa butter plus 5% SSS peak between 0.35 and 0.45 h. It is believed that SSS may co-crystallize with high melting fractions of cocoa butter at early time points. A change in slope was also observed for samples containing LLL, evidenced in Figure 3 as a shoulder to the right side of the crystallization peak (between 0.90 and 1.20 h of crystallization). Such change in heat flow is thought to be indicative of either the crystallization of a second – lower melting – fraction or recrystallization of the existing crystalline phase in a higher liquid fraction environment.

The isothermal crystallization behavior of the studied blends at 24 °C is shown in Figure 4. At this temperature, pure cocoa butter will crystallize fractionally, as evidenced by the presence of two distinct crystallization peaks. The first peak, corresponding to a high melting point fraction, had an onset time of 2.2 h. The second peak, corresponding to a low melting point fraction, had an onset time of 6 h. Upon addition of 1% LLL fractional crystallization is evident as a shoulder to the right of the main crystallization peak forms after roughly 3.9 h. This shoulder corresponds to the crystallization of a lower melting fraction. Further addition of LLL prevented fractionation, as only a single peak was observed. The enrichment of a liquid TAG (i.e., LLL) is believed to increase molecular mobility in the melt, promoting the formation of mixed crystals and thus preventing the fractionation.

A single crystallization event was observed in SSS-enriched cocoa butter crystallized isothermally at 24 °C (Figure 4). The effect of SSS addition on  $\tau$  was found to be somewhat proportional to the amount of SSS added. As the concentration of SSS increases, so does the number of high melting point molecules, which become undercooled (with a melting point of 54.9 °C, at 24 °C SSS has a  $\Delta T$  of roughly 30 °C), thus leading to a larger driving force for nucleation. This resulted in shorter values of  $\tau$ , as well as in co-crystallization of SSS with the bulk of the TAG in cocoa butter, thereby preventing fractional crystallization.

**Crystal Structure.** When liquid oil is cooled to a temperature below its melting point, it will undergo a phase change. The TAGs, which are in random thermal motion in the liquid oil, will orient and align with each other in characteristic lateral packing and longitudinal stacking forming lamellae upon undercooling. Series of lamellae form domains, which in turn stack to form single crystallites.<sup>30,35</sup> Crystallites

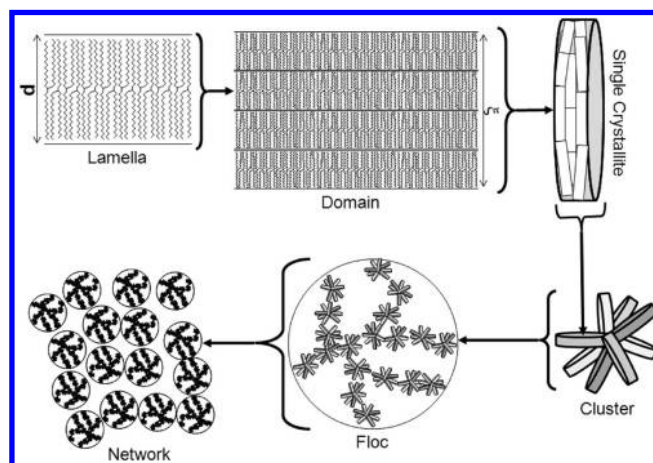


**Figure 5.** Schematic representation of the different levels of structure in crystallized fats. A single crystallite may have one or more domains of a thickness  $\xi$ , composed in turn of several lamellae of thickness  $d$ . Each lamella is formed by TAG organized with a characteristic longitudinal stacking and lateral packing.<sup>35</sup>

aggregate with each other to form clusters, further interacting with each other to create flocs which ultimately form three-dimensional networks.<sup>35,36</sup> Such a hierarchy of network in a fat crystal network is depicted in Figure 5. In our study, the crystalline network formed from cooling cocoa butter blends at 20 and 24 °C was examined by measuring some of these structural levels using powder X-ray diffraction. Wide angle reflections were used to determine the characteristic “short spacings”, which provide information regarding the lateral packing of fatty acid chains within the lamella. Similarly, small angle reflections were used to obtain the long spacings, which correspond to the 001, and higher order planes of the unit cell, which are a function of the size and polymorphic form of the TAGs forming the lamellae. Additionally, the full width half-maximum (fwhm) was used to determine the size of the domains ( $\xi$ ) (Figure 6). fwhm is the width of the long spacing peak at 50% of the total peak amplitude. Furthermore, PLM was used to image the morphology and distribution of the clusters or flocs.

The development of crystalline structures of cocoa butter blends at 20 °C is shown in Figure 7. Diffraction patterns were acquired every 200 s. The first 52 min are illustrated. For each blend, an initial peak with a short spacing of 4.21 Å and a long spacing of 49.21 Å was observed. This crystalline form corresponds to the unstable  $\alpha$  polymorph

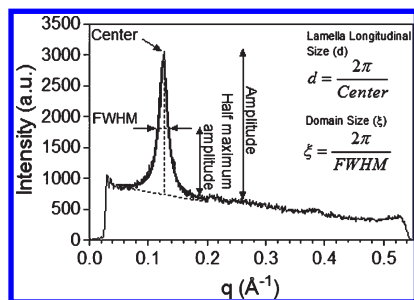


**Figure 6.** A short angle X-ray diffraction pattern, illustrating the parameters obtained which characterize the crystal structure.

(Form II)<sup>13,15</sup> which is characterized by a double chain length structure conformation with no tilt.<sup>35</sup> This crystalline form continues to grow as time progresses. After roughly 30 min a second peak with a short spacing of 4.3 Å, and a long spacing of 45 Å is observed (indicated by the arrows in Figure 7). These spacings point to the crystallization of the metastable  $\beta'$  phase in an inclined (with respect to the lamellar interface) double chain length structure. This peak grows over time, both in the small and the large spacings, indicating an increase in the amount of the  $\beta'$  polymorph. The  $\alpha$  and the  $\beta'$  forms coexist as indicated by the presence of both peaks in the small spacing regions. Conversely, in the large spacings region, the two peaks can be resolved for quite

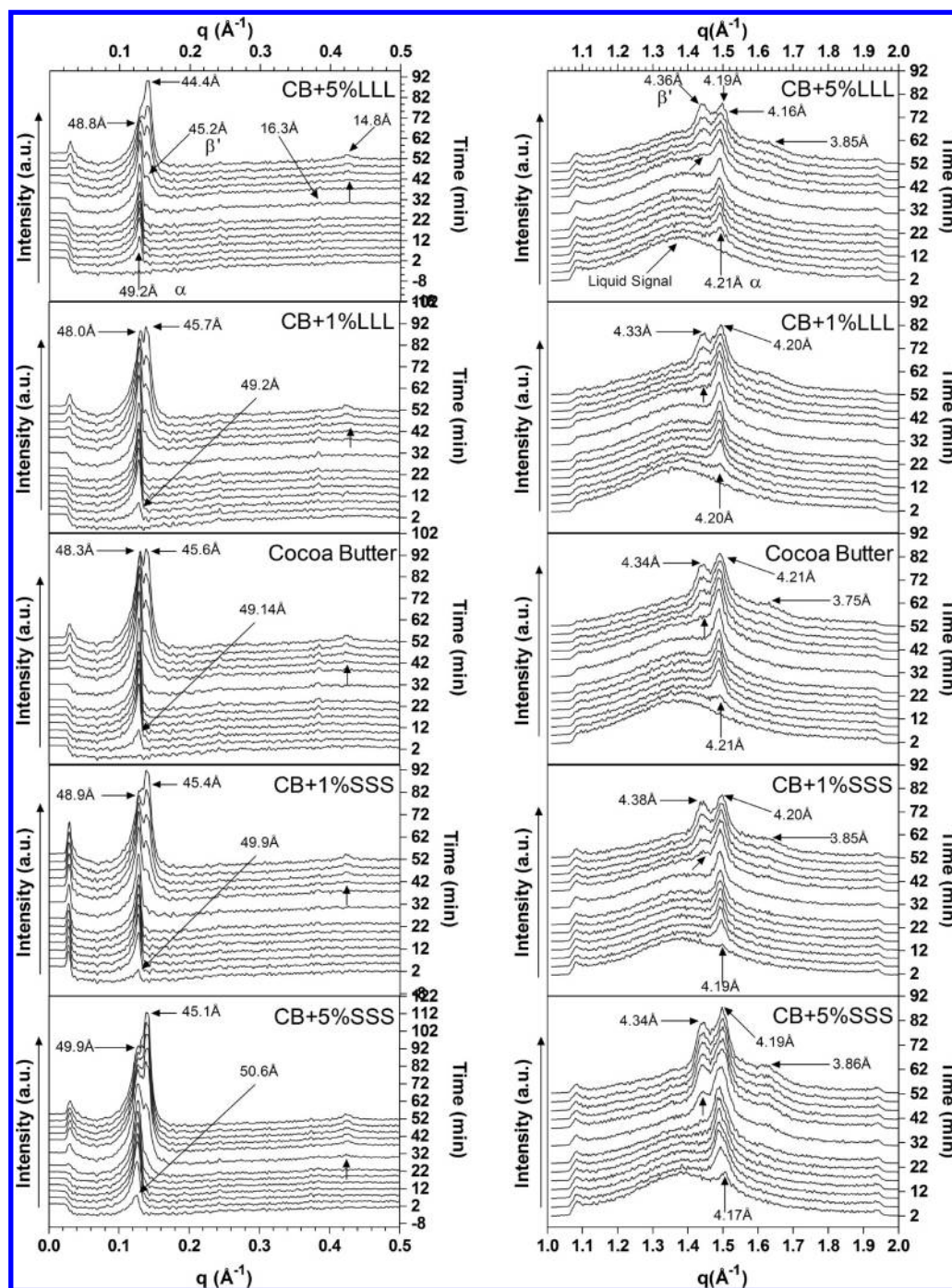


**Figure 7.** XRD patterns of cocoa butter blends crystallized isothermally at 20 °C. Scans were performed every 200 s during a 52 min period. Plots on the left column correspond to the long spacings, while plots on the right column correspond to the short spacings.



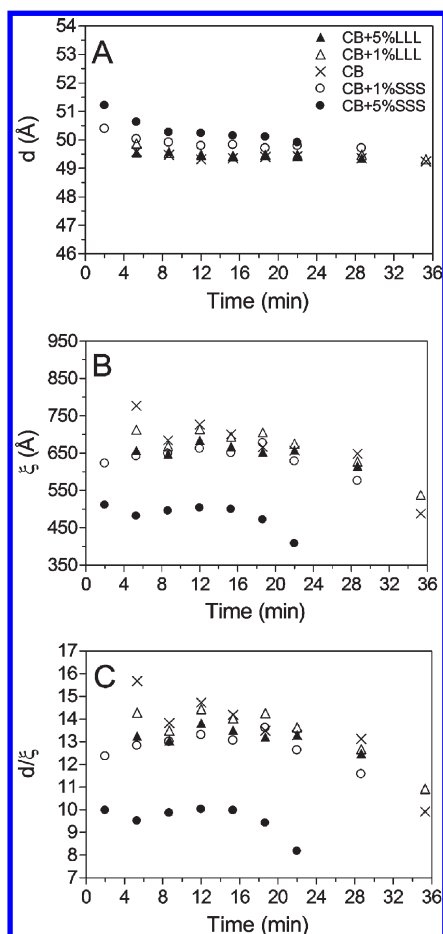


**Figure 8.** Lamellae ( $d$ ) (A), domain ( $\xi$ ) (B) size, and number of lamellae per domain (C) obtained from long spacing peak parameters (peak position and fwhm) of cocoa butter blends crystallized statically at 20 °C for 36 min.

some time. In some blends (cocoa butter enriched with 5% LLL, 1 and 5% SSS), however, the  $\alpha$  peak merges with the  $\beta'$  indicating a possible polymorphic transformation of the  $\alpha$  phase to the  $\beta'$  form.

As previously discussed, the same polymorphic forms are observed in all blends; however, differences are observed in the time of their appearance. In the case of cocoa butter enriched with SSS, a peak is observed as early as 2 min after the sample has reached 20 °C, while for the rest of the samples no evidence of crystallinity was observed until after 5.3 min. Similarly, the second peak with a short spacing of 4.3 Å was observed after 28.6 min for cocoa butter + 5% SSS, while it was not observed until after 35 min for the rest of the blends. This is consistent with the shorter values of  $\tau$  (determined by DSC) previously reported for blends containing the high melting point SSS.

The small angle reflections were further analyzed to obtain structural information regarding the crystals formed. Peaks were fitted to a Lorentzian curve using Prism 4 software (Graph Pad Software Inc., San Diego CA, USA). The center of the peak, as well as the fwhm, were obtained and used to calculate the size of the lamellae ( $d$ ) and the domain size ( $\xi$ ) (Figure 6). Additionally, the number of lamellae per domain were obtained. The results from the diffraction patterns acquired during the first 35 min, when only the  $\alpha$  form is present, are shown in Figure 8. The crystallization of the  $\beta'$  polymorph complicated the analysis, due to the difficulty

in resolving each polymorph's corresponding peaks. As shown in Figure 8, the long spacing for cocoa butter crystallized at 20 °C throughout the first 36 min of crystallization is 49.2 Å. When cocoa butter is enriched with SSS, the lamellae are larger as evidenced by larger long spacings. After 2 min, the initial crystal structure was characterized by long spacings of 50.3 and 51.2 Å for blends with 1% and 5% SSS, respectively. One can visualize the lateral packing of TAG molecules during crystallization and the impact that the chain length and conformation of its constituent lipid species have on the overall interlamellar distance. TAGs in cocoa butter are mainly monounsaturated (i.e., POP, POS, SOS). The double bond of the oleic acid in the sn-2 position of the glycerol backbone translates to a kink in their structure. On the other hand, the fully saturated SSS is a spatially longer molecule (absence of kinks or bends in the stearic acid moieties). As nuclei form, which are believed to be rich in high melting point SSS molecules, the size of the lamellae will be somewhat longer relative to nuclei rich in monounsaturated TAG. In time, the interlamellar distance of SSS containing blends shortens as a result of subsequent inclusion of monounsaturated (shorter) TAG from the melt, being comparable to that of cocoa butter's 49 Å after 8 min for 1% SSS and 22 min for 5% SSS. On the other hand, at these early time points the low melting unsaturated LLL molecules will most likely exist in the melt, having no impact on the crystal structure. This is evidenced by the long spacings of blends with LLL comparable to those of pure cocoa butter.

SSS also affected the size of the domains as evidenced by a dramatic decrease in  $\xi$  for blends of cocoa butter + 5% SSS (Figure 8B). Blends containing 5% SSS have  $\xi$  values almost 200 Å smaller than the rest of the samples, which corresponds to a crystalline domain with 10 vs 14 stacked lamellae (Figure 8C). It appears that the inclusion of SSS in the crystal structure infringes significantly upon the order of the domain. Only small differences were observed among the other samples, with cocoa butter having the highest  $\xi$  values. For all three parameters plotted in Figure 8, there is a relatively constant value from 6 to 20 min, a time period where the  $\alpha$  phase is present. As time reaches the crystallization of the  $\beta'$  phase, the existing crystal structure changes as a result of the formation of this new phase from the melt, along with possible transformation of the  $\alpha$  into the  $\beta'$  forms. This is indicated by dramatic decreases in  $\xi$ , as well as the number of lamellae per domain.

After initial crystallization studies, samples were stored isothermally at 20 °C for further analysis. The diffraction patterns of the studied blends stored for 1, 2, 3, and 7 days are shown in Figure 9. After 1 day of storage, two short spacings at 4.36 and 4.18 Å, and a long spacing at 43.9 Å, were observed for cocoa butter. This crystalline structure corresponds to cocoa butter's  $\beta'$ (IV) polymorph.<sup>12</sup> After 2 days of storage, the same spacings were observed, along with a small peak at 4.58 Å, indicating the presence of the stable  $\beta$  form.<sup>5,15</sup> In time, this 4.58 Å peak grows, while the peaks at 4.36 and 4.18 Å decrease in size. At 20 °C, cocoa butter reaches an equilibrium SFC after only 120 min;<sup>37</sup> thus the formation and growth of the newly observed  $\beta$  phase is thought to be at the expense of the existing  $\beta'$  through solid state polymorphic transformations.<sup>7</sup> The transformation of the  $\beta'$  to the more efficiently packed  $\beta$  results from a structural stabilization of the crystal structure in which the unsaturated fatty acid (oleic) segregates into one chain layer

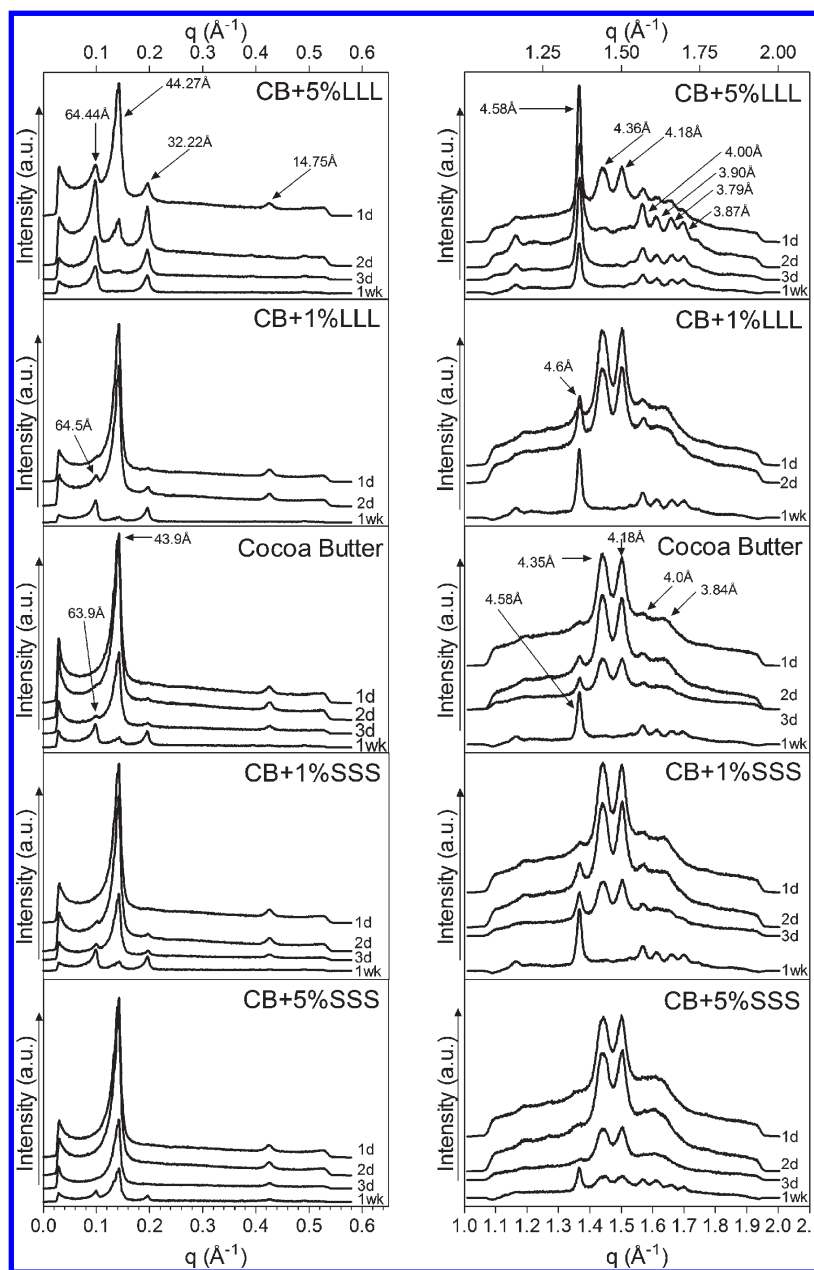


**Figure 9.** XRD patterns of cocoa butter blends crystallized isothermally and stored at 20 °C. Scans were performed after 1, 2, 3, and 7 days of storage. Plots in the left column correspond to the long spacings, while plots on the right column correspond to the short spacings. Signal intensities have been reduced and shifted to avoid overlap.

and the remaining two saturated fatty acids (palmitic and/or stearic) are located in a different layer,<sup>38,39</sup> creating a triple chain length structure. This is evidenced in our work by a change in the long spacing peaks from 43.9 to 63.9 Å after 3 days, corresponding to a 3 L conformation<sup>35</sup> typical of the  $\beta$  form. After one week, the  $\beta'$  peaks have disappeared, and a large  $\beta$  peak (with a short spacing at 4.58 Å) is observed.

Addition of the low melting point LLL molecules to cocoa butter accelerates the formation of the stable  $\beta$  form at 20 °C. The characteristic long spacing of the 3 L conformation at 64.5 Å and the short spacing at 4.6 Å of the stable  $\beta$  form became apparent after only 1 day of storage, and were very pronounced after only 2 days of storage for cocoa butter with 1% LLL. Furthermore, upon addition of 5% LLL, a long spacing at 64.4 Å and a short spacing at 4.58 Å were observed after only 1 day of storage at 20 °C, along with the

reflections associated with the  $\beta'$  form. After only 2 days, a diffraction pattern typical of the  $\beta(V)$  form was observed in the short spacings region. It is believed that LLL promotes the transformation of metastable forms to the stable  $\beta$  form. Our results are consistent with those reported by Smith et al.,<sup>40</sup> which reported that addition of only 1% hazelnut oil to tempered cocoa butter accelerated  $\beta' \rightarrow \beta$  transformation. The presence of liquid oil has also been reported to aid in the polymorphic transformations of other fat systems such as lard<sup>41</sup> and anhydrous milk fat.<sup>42</sup> Similarly, the presence of a low melting fraction in milk fat induced polymorphic transformations in higher melting point fractions.<sup>43,44</sup> Our findings confirm that the presence of liquid oil either entrapped in the crystalline network or on the crystal surface accelerate polymorphic transformations, as molecular diffusion is altered, allowing for TAG to adopt higher stability arrangements.<sup>18,23</sup>

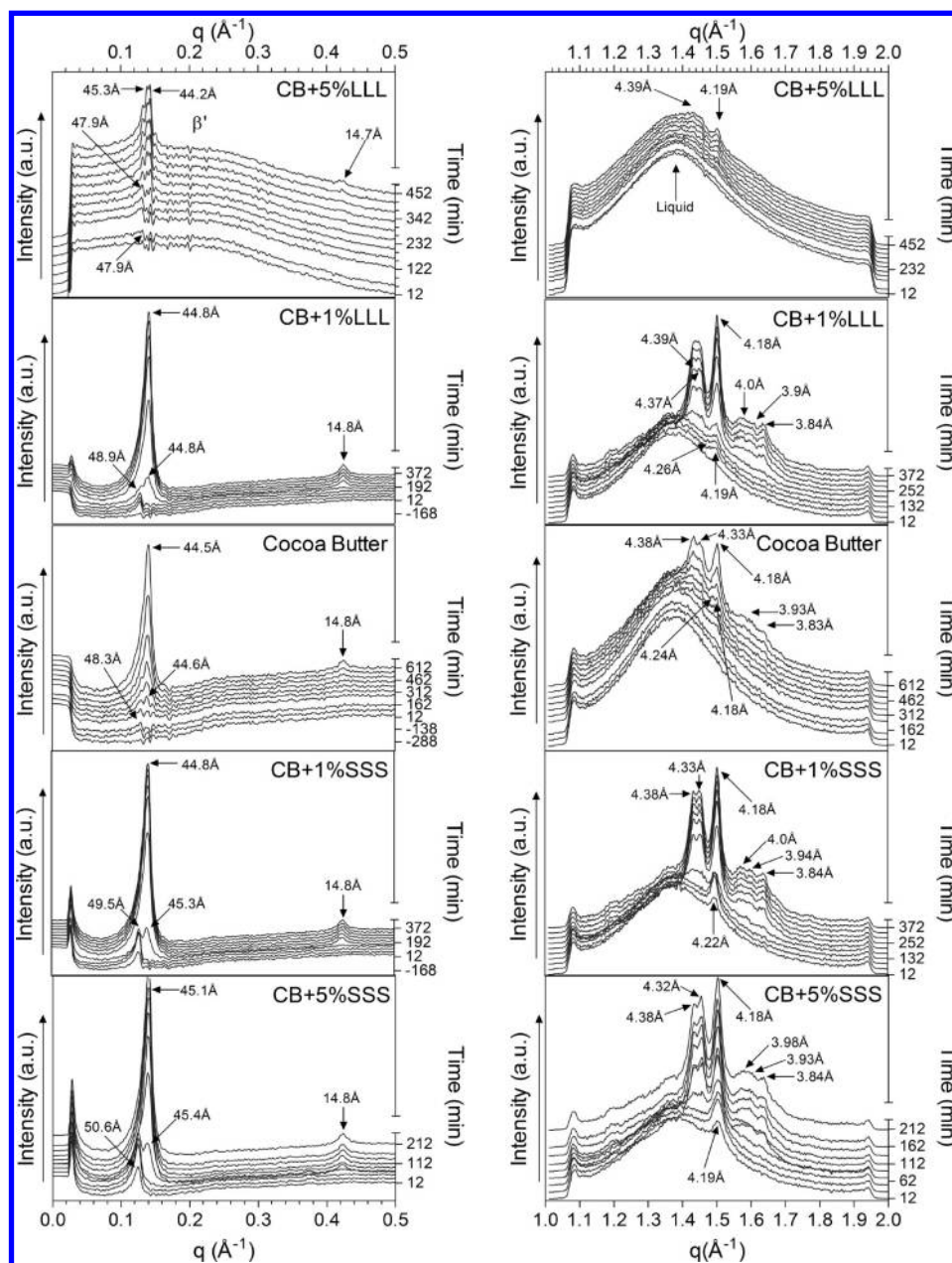


**Figure 10.** XRD patterns of cocoa butter blends crystallized isothermally at 24 °C. Plots on the left column correspond to the long spacings, while plots on the right column correspond to the short spacings.

SSS also affected the polymorphic transformation of the studied blends. Although SSS promoted the early appearance of the metastable forms  $\alpha$  and  $\beta'$ , it decreased the rate of transformation into the stable  $\beta$  form. No differences were observed between cocoa butter and cocoa butter enriched with 1% SSS. Upon addition of 5% SSS, the spacings corresponding to the stable  $\beta$  polymorph were not observed during the first 3 days of storage. It was not until 1 week of storage that a diffraction pattern typical of a  $\beta$  form was observed. As previously mentioned, it is thought that LLL promotes polymorphic transformations as it increases the volume fraction of liquid in the system, thus decreasing viscosity and enhancing molecular mobility. The opposite occurs with addition of SSS. Increase in viscosity of model chocolate melts have been reported in the presence of trisaturated TAG's<sup>45</sup> where high melting molecules,

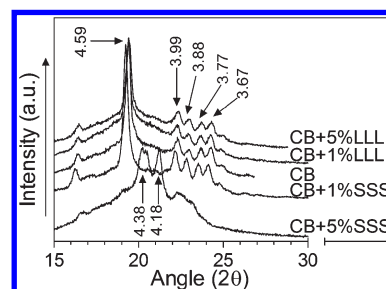


**Figure 11.** XRD short spacing patterns of cocoa butter blends crystallized isothermally at 24 °C for 1 day.

such as SSS, become undercooled and crystallize out. The proposed effect of SSS on melt viscosity results in hindered molecular mobility and thus delayed polymorphic transformations.



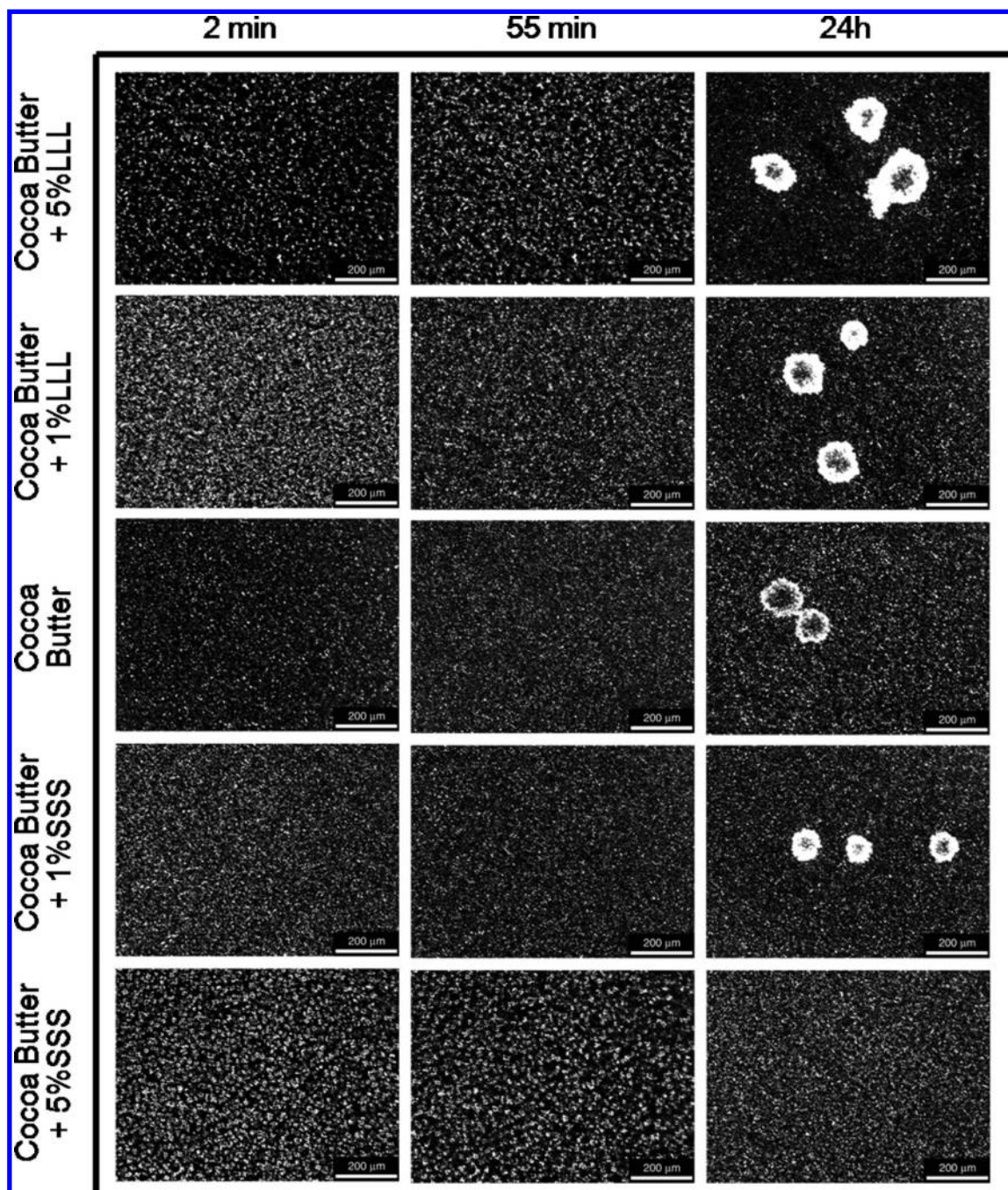


**Figure 12.** Polarized light micrographs of cocoa butter blends crystallized isothermally at 20 °C. Prior to imaging, samples were heated to 80 °C for 20 min, followed by cooling at a rate of 5 °C/min. The microstructure was imaged at different time points.

The polymorphism of cocoa butter blends at 24 °C during the first 12 h of crystallization is illustrated in Figure 10. For all studied blends, the first peak observed in the small angle region had a long spacing between 47.9 and 50.6 Å, corresponding to the metastable  $\alpha$  phase.<sup>35</sup> Consistent with observations at 20 °C, blends with SSS had the highest long spacings for the  $\alpha$  form (49.5 and 50.6 Å for 1% and 5% added SSS, respectively) relative to the rest of the sample blends (between 48.3 Å for pure cocoa butter and 47.9 Å for LLL enriched cocoa butter). In time a second peak was observed with a long spacing between 44 and 45 Å, corresponding to the  $\beta'$  form.<sup>31</sup> The times at which the  $\beta'$  form appeared differed with composition. For blends containing SSS, the  $\beta'$  form was observed after 80 min, for pure cocoa butter after 100 min, and for blends containing LLL after

100–120 min of crystallization. As the  $\beta'$  peak grew in time, the  $\alpha$  peak correspondingly disappeared.

In the wide angle region, small spacings were observed at 4.39, 4.18, 3.9, and 3.8 Å for all samples. On the basis of the work published by Sato and Koyano,<sup>15</sup> the  $\beta'$ (IV) of cocoa butter displays short spacings at 4.35 and 4.15 Å, and a long spacing at roughly 44 Å. Thus, we believe that all samples are in the  $\beta'$  form. Differences were once again found between samples with regard to the times at which the spacings were observed. Blends containing SSS crystallized more rapidly and peaks were observed at earlier times relative to blends with LLL. During the first 12 h of crystallization there was no evidence of the existence of the stable  $\beta$  form.

The polymorphism of blends crystallized at 24 °C was further studied after 24 h of isothermal storage. The resulting



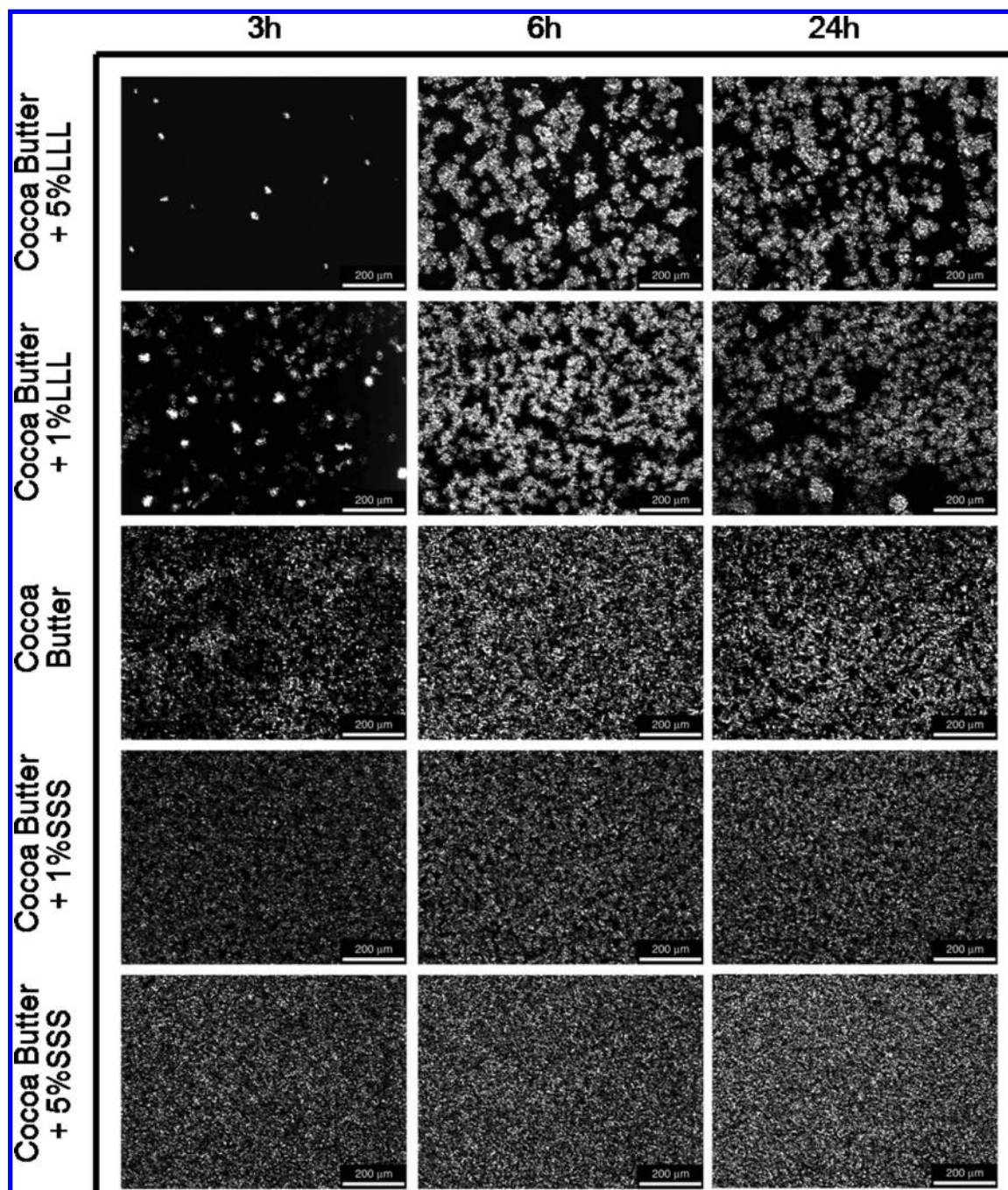


**Figure 13.** Polarized light micrographs of cocoa butter blends crystallized isothermally at 24 °C. Prior to imaging, samples were heated to 80 °C for 20 min, followed by cooling at a rate of 5 °C/min. The microstructure was imaged at different time points.

XRD scans are shown in Figure 11. For all blends except cocoa butter + 5% SSS, a very large peak with spacing at 4.59 Å was observed, along with smaller spacings at 3.99, 3.88, 3.77, and 3.67 Å. This diffraction pattern corresponds to the stable  $\beta(V)$  form of cocoa butter.<sup>14</sup> On the other hand, cocoa butter + 5% SSS had spacings at 4.38 and 4.18 Å that correspond to a metastable  $\beta'$  form. Consistent with the results observed at 20 °C, the addition of high melting SSS was found to delay polymorphic transformations of the less stable forms to the stable  $\beta$  form in spite of it reducing the induction times of crystallization of the unstable forms.

**Microstructure.** The microstructure of the fat crystal networks that formed at 20 and 24 °C was imaged using

PLM. This allows for the study of the crystalline microstructure, yet at a much larger length-scale relative to XRD, enabling the visualization of the aggregation of domains into single crystallites and their further aggregation into clusters.

When crystallized at 20 °C, a large number of crystallites were formed after only 2 min in all blends, as shown in Figure 12. The observed crystal morphology can be described as a high number of very small needle-like crystallites. At this time–temperature condition, cocoa butter crystallized in the  $\alpha$  polymorph has been reported to yield needle-like features.<sup>9</sup> No differences were observed in the first hour of crystallization between the studied blends. After 24 h of storage at 20 °C, differences in the microstructure

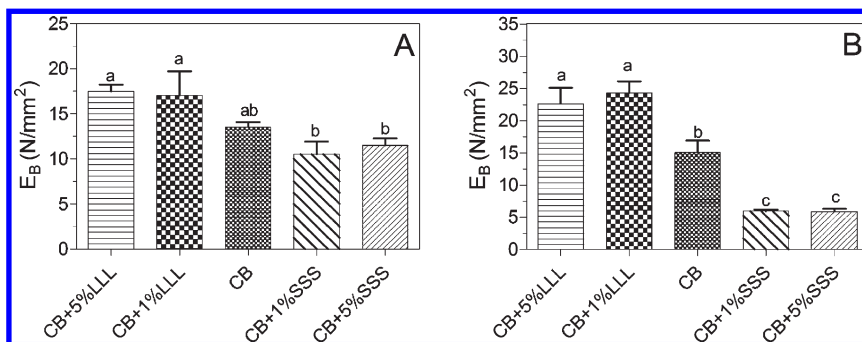


**Figure 14.** Elastic bending modulus ( $E_B$ ) of cocoa butter blends crystallized at 20 °C for 24 h (A) and 24 °C for 48 h (B). Bars represent an average of four replicates. Letters denote significance between samples at each crystallization temperature ( $P < 0.05$ ).

**Table 1. Structural Parameters Obtained Experimentally or Theoretically from Cocoa Butter Blends at 24 °C**

blend	$\delta$ (J/m <sup>2</sup> )	$\tau$ (h)	$\Delta G_n$ (kJ)	SFC <sub>max</sub> (%)	$D_b$	eq diam ( $\mu$ m)	displacement (mm)	$F_{fracture}$ (N)	$E_B$ (N/mm <sup>2</sup> )
CB+5%LLL	0.0017	2.50	4.14	49.08	1.79	2.33	0.25	8.58	22.62
CB+1%LLL	0.0019	2.49	3.88	52.14	1.76	2.33	0.26	9.17	24.29
CB	0.0017	2.20	3.54	52.75	1.86	2.16	0.47	10.27	15.09
CB+1%SSS	0.0014	1.64	2.94	50.74	1.90	1.82	0.42	3.80	5.97
CB+5%SSS	0.0013	0.74	2.26	56.18	1.88	1.82	0.42	3.69	5.84

were observed. The presence of relatively big crystal clusters, which are 100–200  $\mu$ m in size, was evident for all sample blends except for cocoa butter + 5% SSS. Aggregation of crystallites into clusters has been observed for cocoa butter in the  $\beta'$  polymorph, which has been formed via the  $\alpha$  phase between 15 to 22 °C.<sup>9</sup> The presence of clusters is evidence of a polymorphic transformation and we have shown that SSS delays polymorphic transformation; therefore, cocoa butter + 5% SSS is expected to be the last blend to display such changes in crystal morphology.

The imaged microstructures of samples crystallized at 24 °C are shown in Figure 13. After 3 h of crystallization, the morphology of cocoa butter crystals consisted of very small, needle-like crystalline structures. In time, the crystalline mass increased; however, no changes in crystal morphology were observed during the initial 24 h. Addition of LLL considerably impacted the microstructure of cocoa butter, as evidenced by larger features surrounded by substantial amounts of liquid oil. A concentration effect was observed, as the number of features decreased in blends with higher amounts of LLL. In time, the solid fraction increased; yet after 24 h of storage considerable areas void of solid mass were still present. In some cases this “empty space” was filled by liquid oil. However, segregation within the microscope slide was observed with the naked eye at 5% LLL. Contrary to the effect of LLL, the addition of SSS to cocoa butter increases the crystallization rate, resulting in a higher number of small crystallites observed throughout the entire field of view. No significant changes in the microstructure were observed in the time frame of this study (i.e., 3–24 h).

**Mechanical Properties.** The effects of SSS and LLL addition to cocoa butter’s mechanical strength was determined by quantifying the elastic bending moduli ( $E_B$ ) for samples crystallized at 20 and 24 °C (Figure 14). The addition of SSS increased the solid fraction of cocoa butter, yet resulted in a softening effect, while LLL increased its mechanical strength. The observed outcome on  $E_B$  can be explained in terms of the effect that the addition of different molecules has on the crystal–melt interfacial tension ( $\delta$ ). A theoretical estimation of  $\delta$  was obtained from a derivation of the

Fisher–Turnbull equation,<sup>46</sup> in its following form:

$$\delta = \left( \frac{3mk_B\Delta H_f^2}{16\pi(V_m^s)^2T_f^2} \right)^{1/3} \quad (3)$$

where  $m$  ( $K^3$ ) is the slope of a  $\ln(\tau T)$  vs  $1/[T(\Delta T)^2]$  plot constructed with  $\tau$  values obtained from experimental calorimetric data (Figures 3 and 4);  $k_B$  is the Boltzmann constant ( $1.38 \times 10^{-23}$  J/K);  $\Delta H_f$  (J/mol) is the enthalpy of fusion obtained from experimental calorimetric data;  $V_m^s$  ( $m^3/mol$ ) is the molar volume of solid fat calculated as the ratio of cocoa butter’s average molecular weight divided by its density; and  $T_f$  (K) is the melting temperature also obtained experimentally from calorimetric data. The molecular weight of POS (861.4 g/mol) was considered the average molecular weight of cocoa butter. Table 1 shows the calculated  $\delta$  as well as free energies of nucleation ( $\Delta G_n$ ) at 24 °C for all studied blends.  $\Delta G_n$  values were calculated using the following:<sup>47</sup>

$$\Delta G_n = \frac{mk_B}{\Delta T^2} \quad (4)$$

The relationship between  $\delta$  and the mechanical strength of fat crystal networks is expressed in the model proposed by Marangoni<sup>34,48</sup> and Marangoni and Rogers,<sup>49</sup> which describes the estimation of the modulus of elasticity ( $E$ ) with the following equation:

$$E = \frac{\sigma^*}{\varepsilon^*} \sim \frac{6\delta}{a\varepsilon^*} \Phi^{1/d-D} \quad (5)$$

where  $\sigma^*$  and  $\varepsilon^*$  are the critical stress and strain, respectively;  $a$  is the size of the particles that form the network;  $\Phi$  is the solid fraction; and  $d$  and  $D$  are the Euclidean dimension of the embedding space ( $d = 3$ ), and the fractal dimensions, respectively. The above expression illustrates that the elastic properties of a fat crystal network will depend on the amount of mass present (indicated by  $\Phi$ ), the particle properties ( $a$ ), and the interaction between these particles (associated with  $\delta$ ). Throughout this work, a series of structural indicators have been experimentally obtained, such as the SFC (%); parameters that describe the microstructure (i.e., number of features ( $a$ ) and fractal dimension ( $D_b$ )); and the large



deformation properties of the studied blends (displacement to point of fracture and  $E_B$ ). These are also shown in Table 1.

The addition of high melting point SSS to cocoa butter changes the saturation conditions in the melt, which result in lower  $\Delta G_n$ , translating into lower inductions times (Figures 2–4). Slight increases (up to 7% at 24 °C) were observed in the SFC, alongside decreased particle size (roughly 16%) with small changes in  $D_b$ . This would point toward an expected increase in the elasticity of the network. However, a reduction of approximately 20% in the  $\delta$  was observed at higher SSS contents. The effect of  $\delta$  on  $\sigma^*$  of cocoa butter over a range of solids' fractions was simulated according to eq 5, using the structural parameters obtained experimentally throughout this work. Averages of the equivalent

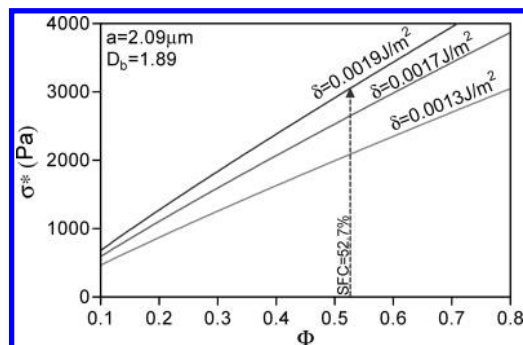


**Figure 15.** Simulation of the effect of surface free energy on the critical stress ( $\sigma^*$ ) of a plastic disperse system over a range of solids' volume fraction, which is based on the model proposed by Marangoni and Rogers (2003).<sup>49</sup> The primary particle diameter ( $a$ ) and fractal dimension ( $D_b$ ) used for this simulation were the average of the equivalent particle diameter and  $D_b$  (obtained from the analysis of polarized light micrographs acquired at 24 °C) of the five studied cocoa butter sample blends. The SFC(%) of pure cocoa butter crystallized isothermally at 24 °C is indicated. The chosen surface free energy values for this simulation correspond to that of pure cocoa butter (0.0017 J/m<sup>2</sup>), as well as cocoa butter enriched with LLL (0.0019 J/m<sup>2</sup>) and SSS (0.0013 J/m<sup>2</sup>).

particle diameter (2.09  $\mu\text{m}$ ) and  $D_b$  (1.89) for all studied blends were used as set parameters. Plots for  $\sigma^*$  as a function of  $\phi$  at the highest (1% LLL), intermediate (pure cocoa butter), and lowest (5% SSS) values for  $\delta$  were calculated. It is illustrated in Figure 15 that at a particular solid fraction (i.e., 52.7% SFC for cocoa butter) the  $\sigma^*$  decreases proportionally (from 2645 Pa to 2084 Pa) when  $\delta$  decreases roughly 20% upon addition of SSS. Such a decline in  $\sigma^*$  will result, according to eq 4, in a decrease in the elasticity of the system, as observed in experimental values of  $E_B$ . Likewise, the calculated increases in  $\delta$  for blends containing LLL will result in higher  $\sigma^*$ , yielding a crystal network with higher  $E_B$ .

In addition to the structural parameters previously discussed, polymorphism also affects the mechanical properties of the studied blends. The addition of LLL accelerated the  $\beta' \rightarrow \beta$  transformation, while SSS slowed down such transformations. It has been demonstrated by Brunello et al.,<sup>50</sup> that polymorphism strongly influences the mechanical properties of cocoa butter. The  $\beta$  polymorph is not only the most stable but also the most efficiently packed and most dense crystal form. As SSS delays the  $\beta' \rightarrow \beta$  transformation, it is then expected that samples which contain SSS will be softer relative to those in which the transformation into the  $\beta$  form has been completed.

## Conclusions

This work has proven that significant alteration to the crystal structure and ergo the functionality of cocoa butter can be achieved through minor changes in its TAG composition, as depicted in Figure 16. Addition of SSS changed the saturation conditions of the melt, consequently affecting crystallization and the resulting crystal network. The high melting point saturated TAGs become rapidly undercooled as the temperature of cocoa butter decreases, providing the energy required for nucleation and crystal growth (observed as lower onset crystallization temperatures and onset times for crystallization). Fully saturated SSS molecules are spatially

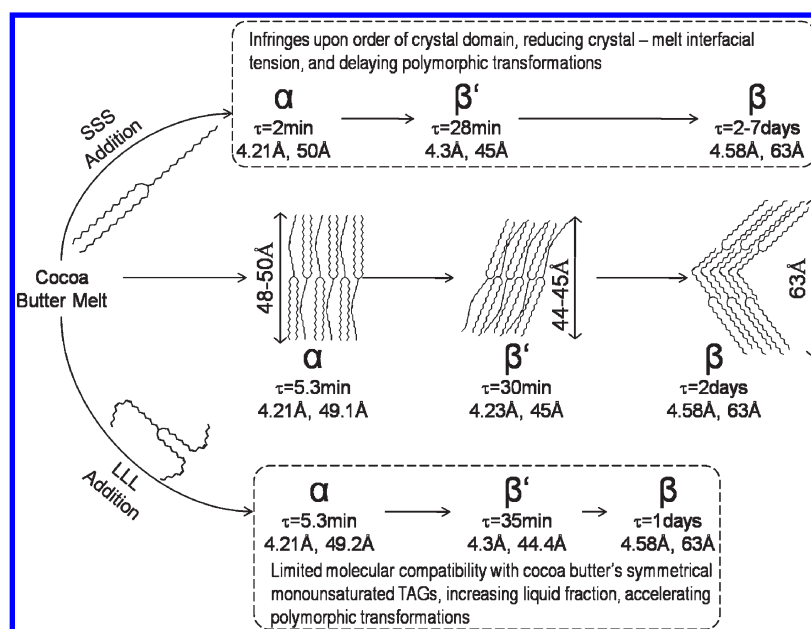


**Figure 16.** Schematic representation of cocoa butter's crystallization, in its native state and upon addition of either saturated tristearin (SSS) or unsaturated trilinoleate (LLL) at 20 °C. Indicated are times ( $\tau$ ) in which each polymorphic form was observed with X-ray diffraction, as well as their short and long spacings.

bigger (i.e., straight) relative to monounsaturated TAGs which have bends in the unsaturated oleic acid moieties. Their inclusion into the crystal lattice of nuclei introduces a certain degree of disorganization during the stacking of lamella in the very early stages of crystallization, thus resulting in differences in crystal lamella and domain size. Subsequently, different levels of structure are affected. Despite the lower induction times for crystallization observed, SSS delayed polymorphic transformation from metastable forms into the stable  $\beta$  form. Lastly, cocoa butter with added SSS was found to be less elastic, as a result of the effect that SSS had on the crystal–melt interfacial tension.

Changes in the TAG profile of cocoa butter in the opposite direction (i.e., addition of fully unsaturated LLL) likewise resulted in structural differences. With a very low melting point, LLL will not be undercooled at the studied temperatures, and will only slightly affect induction times and temperatures of crystallization. No significant changes in the size of the lamellae were observed. This, along with LLL's structural incompatibility with the crystal surface suggests that LLL does not co-crystallize with the bulk of cocoa butter's TAGs, but rather surrounds crystal domains, increasing the crystal network's liquid fraction. Consequently, LLL enhances molecular mobility and the rearrangement of TAG molecules into highly dense, efficiently packed, stable crystalline structures (in other works, accelerates  $\beta' \rightarrow \beta$  transformation).

**Acknowledgment.** In memory of Professor Michel Ollivon. The execution of these experiment and analysis would not have been possible without his generosity, support, and scientific insight.

## References

- (1) Narine, S. S.; Marangoni, A. G. Structure and mechanical properties of fat crystal networks. In *Physical Properties of Lipids*; Marangoni, A. G.; Narine, S. S., Eds.; Marcel Dekker: New York, NY, USA, 2002; pp 63–84.
- (2) Campos, R.; Narine, S. S.; Marangoni, A. G. *Food Res. Int.* **2002**, *35*, 1971–1982.
- (3) Dimick, P. S. Compositional effect on crystallization of cocoa butter. In *Physical Properties of Fats, Oils, and Emulsifiers*; Widlak, N., Ed.; AOCS Press: Champaign, IL, USA, 2000; pp 140–162.
- (4) Lipp, M.; Simoneau, C.; Ulberth, F.; Anklam, E.; Crews, C.; Brereton, P.; de Greyt, W.; Schwack, W.; Wiedmaier, C. *J. Food Compos. Anal.* **2001**, *14*, 399–408.
- (5) Wille, R. L.; Lutton, E. S. *J. Am. Oil Chem. Soc.* **1996**, *43*, 491–496.
- (6) van Malssen, K.; Peschar, R.; Schenk, H. *J. Am. Oil Chem. Soc.* **1996**, *73*, 1209–1215.
- (7) van Malssen, K.; van Langevelde, A.; Peschar, R.; Schenk, H. *J. Am. Oil Chem. Soc.* **1999**, *76*, 669–676.
- (8) Manning, D. M.; Dimick, P. S. *Food Microstruct.* **1985**, *4*, 249–265.
- (9) Marangoni, A. G.; McGauley, S. E. *Crys. Growth Des.* **2003**, *3*, 95–108.
- (10) Beckett, S. T. *The Science of Chocolate*; Royal Society of Chemistry Paperbacks: Cambridge, UK; 2000.
- (11) Rousset, Ph.; Rappaz, M. Experimental study and computer modeling of the dynamic and static crystallization of cocoa butter. In *Crystallization and Solidification Properties of Lipids*; Widlak, N.; Hartel, R. W.; Narine, S. S.; AOCS Press: Champaign, IL, USA; pp 96–109.
- (12) Mazzanti, G.; Guthrie, S. E.; Sirota, E. B.; Marangoni, A. G.; Idziak, S. H. J. Crystallization of bulk fats under shear. In *Soft Materials: Structure and Dynamics*; Dutcher, J. R.; Marangoni, A. G., Eds.; Marcel Dekker: New York, USA, 2005; pp 279–298.
- (13) Sato, K.; Arishima, T.; Wang, Z. H.; Ojima, W. K.; Sagi, N.; Mori, H. *J. Am. Oil Chem. Soc.* **1989**, *66*, 664–674.
- (14) Koyano, T.; Hachiya, I.; Arishima, T.; Sato, K.; Sagi, N. *J. Am. Oil Chem. Soc.* **1989**, *66*, 675–679.
- (15) Sato, K.; Koyano, T. Crystallization properties of cocoa butter. In *Crystallization Processes in Fats and Lipid Systems*; Garti, N.; Sato, K., Eds.; Marcel Dekker: New York, NY, USA, 2001; pp 429–456.
- (16) Ng, W. L. *J. Am. Oil Chem. Soc.* **1989**, *66*, 1103–1106.
- (17) Minato, A.; Ueno, S.; Yano, J.; Wang, Z. H.; Seto, H.; Amemiya, Y.; Sato, K. *J. Am. Oil Chem. Soc.* **1996**, *73*, 1567–1572.
- (18) Smith, K.; Cain, F. W.; Talbot, G. *Eur. J. Lipid Sci. Technol.* **2005**, *10*, 683–593.
- (19) Miura, S.; Konishi, H. *Eur. J. Lipid Sci. Technol.* **2001**, *103*, 804–809.
- (20) Lovegren, N. V.; Fray, M. S.; Feuge, R. O. *J. Am. Oil Chem. Soc.* **1976**, *53*, 83–88.
- (21) Gordon, M. H.; Padley, F. B.; Timms, R. E. *Fette Seifen Anstrichmittel* **1979**, *81*, 116–121.
- (22) Timms, R. E. *Confectionery Fats Handbook*; Lipid Technology: Bridgewater, England, 2003; pp 255–269.
- (23) Lovegren, N. V.; Gray, M. S.; Feuge, R. O. *J. Am. Oil Chem. Soc.* **1976**, *53*, 108–112.
- (24) Perez-Martinez, D.; Alvarez-Salas, C.; Morales-Rueda, J. A.; Toro-Vazquez, J. F.; Charo-Alonso, M.; Dibildox-Alvarado, E. *J. Am. Oil Chem. Soc.* **2005**, *82*, 471–479.
- (25) Perez-Martinez, D.; Alvarez-Salas, C.; Charo-Alonso, M.; Dibildox-Alvarado, E.; Toro-Vazquez, J. F. *Food Res. Int.* **2007**, *40*, 47–62.
- (26) Martini, S.; Herrera, M. L.; Hartel, R. W. *J. Agric. Food Chem.* **2001**, *49*, 3223–3229.
- (27) Humphrey, K. L.; Moquin, P. H. L.; Narine, S. S. *J. Am. Oil Chem. Soc.* **2003**, *80*, 1175–1182.
- (28) Toro-Vazquez, J. F.; Gallegos-Infante, A. *J. Am. Oil Chem. Soc.* **1996**, *73*, 1237–1246.
- (29) Dibildox-Alvarado, E.; Toro-Vazquez, J. F. *J. Am. Oil Chem. Soc.* **1989**, *75*, 73–76.
- (30) Fairley, P.; Krochta, J. M.; German, J. B. *J. Am. Oil Chem. Soc.* **1995**, *72*, 693–697.
- (31) Ollivon, M.; Keller, G.; Bourgaux, C.; Kalnin, D.; Villeneuve, P.; Lesieur, P. *J. Ther. Anal. Calorim.* **2006**, *85*, 219–224.
- (32) Steffe, J. F. *Rheological Methods in Food Process Engineering*; Freeman Press: Michigan, USA, 1996; pp 9–10.
- (33) Small, D. M. The physical chemistry of lipids: From alkanes to phospholipids. *Handbook of Lipid Research*; Plenum Press: New York, USA, 1986; Vol. 4.
- (34) Van Malssen, K. F.; Peschar, R.; Schenk, H. *Voedings Middelen Technol.* **1995**, *30*, 67–69.
- (35) Mazzanti, G. *X-Ray Diffraction Study on the Crystallization of Fats under Shear*; University of Guelph: Guelph, ON, Canada, 2004.
- (36) Marangoni, A. G. Crystallography. In *Fat Crystal Networks*; Marangoni, A. G., Ed.; Marcel Dekker: New York, NY, USA, 2005; pp 1–20.
- (37) Campos, R. *Effects of Processing Conditions on the Crystallization of Cocoa Butter*; University of Guelph: Guelph, ON, Canada, 2006.
- (38) Larson, K. *Lipids-Molecular Organization, Physical Functions and Technical Applications*; The Oily Press LTD: Sweden, 1994.
- (39) Sato, K. Molecular aspects in fat polymorphism. In *Crystallization and Solidification Properties of Lipids*; Widlak, N.; Hartel, R. W.; Narine, S. S., Eds.; AOCS Press: Champaign IL, USA, 2001; pp 1–15.
- (40) Smith, K.; Cain, F.; Talbot, G. *Food Chem.* **2007**, *102*, 656–663.
- (41) Rousseau, D.; Marangoni, A. G.; Jeffrey, K. R. *J. Am. Oil Chem. Soc.* **1998**, *12*, 1833–1839.
- (42) Wright, A. J.; Batte, H. D.; Marangoni, A. G. *J. Dairy Sci.* **2005**, *1955*–1965.
- (43) Timms, R. E. *Aust. J. Dairy Technol.* **1980**, 47–53.
- (44) Cisneros, A.; Mazzanti, G.; Campos, R.; Marangoni, A. G. *J. Agric. Food Chem.* **2006**, 6030–6033.
- (45) Cebula, D. J.; Dilley, K. M.; Smith, K. W. *Manufactur. Confectioner* **1991**, *71*, 131–136.
- (46) Marangoni, A. G. The yield stress and elastic modulus of a fat crystal network. In *Fat Crystal Networks*; Marangoni, A. G., Ed.; Marcel Dekker: New York, NY, USA, 2005; pp 255–266.
- (47) Marangoni, A. G. Crystallization kinetics. In *Fat Crystal Networks*; Marangoni, A. G., Ed.; Marcel Dekker: New York, NY, USA, 2005; pp 21–82.
- (48) Marangoni, A. G. *Phys. Rev. B.* **2000**, *21*, 13951–13951.
- (49) Marangoni, A. G.; Rogers, M. A. *Appl. Phys. Lett.* **2003**, *19*, 3239–3241.
- (50) Brunello, N.; McGauley, S. E.; Marangoni, A. G. *Lebensm.-Wiss. Technol.* **2003**, 525–532.